



Journal of Applied and Computational Mechanics



Research Paper

Numerical Simulations of Spoiler's Effect on a Hatchback and a Sedan Car Exposed to Crosswind Effect

Reza Bahoosh¹, Milad Rohani², Mohammad Reza Saffarian³

¹ Department of Mechanical Engineering, Shahid Chamran University of Ahvaz, Ahvaz, Iran, Email: Iran, bahoosh@scu.ac.ir

² Department of Mechanical Engineering, Shahid Chamran University of Ahvaz, Ahvaz, Iran, Email: m-rohani@stu.scu.ac.ir

³ Department of Mechanical Engineering, Shahid Chamran University of Ahvaz, Ahvaz, Iran, Email: mr.saffarian@scu.ac.ir

Received April 26 2021; Revised November 29 2021; Accepted for publication November 30 2021.

Corresponding author: R. Bahoosh (bahoosh@scu.ac.ir)

© 2022 Published by Shahid Chamran University of Ahvaz

Abstract. Numerical simulations of the airflow around a hatchback and a sedan vehicle without and with spoilers are carried out, besides, its effect on drag and lift coefficients are investigated with and without crosswinds. The effects of crosswind on aerodynamic forces are considered and its results are compared with the case without considering the effects of crosswind. For this purpose, the steady-state three-dimensional Navier-Stokes equations are solved by the Simple Method. Moreover, for turbulence modeling, the Realizable $k-\epsilon$ model is implemented. The spoiler angle and its length are changed for both car models; furthermore, the effects of two spoilers on drag and lift coefficients are investigated in detail. All cases are simulated with and without crosswind. The results show that the impact of the spoiler for without crosswind conditions to decrease the lift coefficient in both models is significant; in addition, the drag coefficients are reduced for some cars. It can be concluded that the increase of spoiler length for both sedan and hatchback vehicles can increase the downward force and vehicle stability.

Keywords: Drag coefficient; Lift coefficient; Spoiler; Numerical solution; Crosswind.

1. Introduction

During a car's journey, a significant amount of total energy is consumed to overcome the aerodynamic drag force, consequently, reducing aerodynamic drag forces is one of the ways to save fuel [1]. The relationship between reducing fuel consumption and drag forces is not the same for different speeds [2-3]. The aerodynamics of a car can be affected by adding some features such as a spoiler. One of the features of the spoiler is its impact on the downward force and stability of the car [4-6]. The downward force can improve the performance of racing cars, which is why designers, use the spoiler to produce aerodynamic downward forces [7]. Ahmed et al [8] experimentally studied a basic ground vehicle type of a bluff body (Ahmed body). Crabtree [9], showed that a change in the rear of a vehicle body is an important factor for the aerodynamic characteristics of the vehicle, including drag and lift coefficients. Ranzenbach et al. [10] obtained the effects of wings on bodies of two conventional shapes of racing cars; a three-dimensional simulation with wind tunnel test was conducted. Kim [11], gained the effects of a rear spoiler on a commercial bus. Kieffer et al. [12], conducted a numerical study with the use of the Star-CD code. They considered a ground effect of a front wing, then placed a rear wing at different angles and introduced an angle as the optimal aerodynamic angle for the wing. Fares [13] studied flow over Ahmed's body with the lattice Boltzmann model. Hargreaves et al. [14] investigated the effects of side wind on a trailer, numerically. Chainani and Perera [15], utilized various techniques to redesign and optimize the aerodynamics characteristic of a racing car. Tsai et al. [16], examined numerically the effects of several spoilers with two wings on the stability and aerodynamics noise of a car. Mitra [17] investigated the effects of adding some parts such as a spoiler on a body of a sedan car in an experimental study. Tsubokira et al. [18] reported an effect of transient lateral wind on a simple model of a hatchback car. Hu and Wong [19], investigated numerically an effect of the shape of a spoiler on a passenger car. Zhu et al. [20] accomplished the results of wind tunnel tests to determine the aerodynamic coefficient of four types of road vehicles that were on a conventional bridge deck. Sadettin H. et al. [21] reviewed the effect of a rear spoiler geometry on the car aerodynamics by comparing results of CFD analysis with wind tunnel test. Sung et al. [22] obtained the coefficient of drag and lift for a simple car model at different yaw and pitch angle. Bahoosh et al. [23] investigated numerically the aerodynamics effects of two tandem cars; their results showed that the drag force on each two tandem cars is less than a single car. Cheng and Mansor [24], obtained the effects of a rear spoiler on a hatchback car. Liu et al. [25] carried out experiments on various car models under different flow conditions, including turbulent flow and boundary-layer flow in a tunnel. Mashud and Das [26], examined the effect of angle changing for spoilers at different speeds. Zhang et al. [27] simulated the flow around trains with different computational fluid dynamic (CFD) techniques. Ferraris et al [28] studied the reduction of a city-car prototype's aerodynamic resistance utilizing standard aerodynamic devices, experimentally and numerically. Yildiz and Dandil [29] examined numerically the impact of grilles in a car on the aerodynamic drag coefficient and reduced energy consumption. In this research, the grill is placed horizontally in front of the car. Guo et al. [30] studied the impact of a rear wing on automotive



aerodynamics. In this study, the aerodynamics manner of seven different positions of the rear wing compared with the same angle of attack. They found that due to the rear wing adjustment, the vortices at the top and rear of the car decreased, thus increasing the car pressure and drag coefficient. Shakti et al. [31] compute and improve aerodynamic force on Sedans utilizing a rear spoiler. So they can get better fuel consumption and stability when driving on the road, and also find the noise of wind on the car. Džijan et al. [32] developed a computational model to examine the aerodynamic forces of a closed-wheel race car. The particular focus of this model was to investigate the effects of ground clearance and rake angle on aerodynamic drag and lift forces. The computational results indicate the high impact of the ground clearance and rake angle on the aerodynamic loading of a racing car.

In this research, the airflow is simulated around two models of hatchback and sedan cars by solving governing equations in the form of three-dimensional and steady-state flow; the realizable $k-\varepsilon$ turbulence model was utilized for modeling the turbulent effect; the method of discretization is finite volume method. For evaluating the results of numerical simulation, the aerodynamic features around the Ahmed body [8] are extracted and compared with the available experimental data. After that, the effect of angle and length of spoiler on both car models are studied; moreover, the effects of the simultaneous presence of two spoilers are studied for both models. In addition, the lateral wind effects for all considered simulated models are studied.

2. Geometry of Models

Two models of Volkswagen Golf V, 2008 [33] as a hatchback car and Volkswagen Jetta III, 1993 [34] as a sedan car are shown in figures 1a and 1b; the geometry of these cars are modeled in Solidworks software. Dimensions of both models are given in Table 1. The base length and height of the spoiler are 300 mm and 50 mm, respectively. For reducing the computational time, half of the models are simulated.

The dimensions of the numerical wind tunnel are listed in table 1; according to this, the vehicle's distance to the beginning of the wind tunnel and the end of it are 10,000 mm and 30,000 mm, respectively and the distance to side space around the car (its sides and above it) is 3000 mm.

3. Governing Equations

The continuity and Reynolds averaged Navier-Stokes equations are utilized to solve the flow in the computational domain [35]:

$$\frac{\partial \bar{u}_i}{\partial x_i} = 0 \quad (1)$$

$$\rho \bar{u}_j \frac{\partial \bar{u}_i}{\partial x_j} = \frac{\partial}{\partial x_j} [-\bar{P} \delta_{ij} + 2\mu \bar{S}_{ij} - \rho \bar{u}_i \bar{u}_j] \quad (2)$$

Equation (2), is the Reynolds stress term that should be modeled. For this purpose, the Realizable $k-\varepsilon$ turbulence model is utilized [36]:

$$\frac{\partial}{\partial x_j} (\rho k \bar{u}_j) = \frac{\partial}{\partial x_j} \left[\left(\mu + \frac{\mu_t}{\sigma_k} \right) \frac{\partial k}{\partial x_j} \right] + P_k - \rho \varepsilon \quad (3)$$

$$\frac{\partial}{\partial x_j} (\rho \varepsilon \bar{u}_j) = \frac{\partial}{\partial x_j} \left[\left(\mu + \frac{\mu_t}{\sigma_\varepsilon} \right) \frac{\partial \varepsilon}{\partial x_j} \right] + \rho C_1 S_\varepsilon - \rho C_2 \frac{\varepsilon^2}{k + \sqrt{\nu \varepsilon}} \quad (4)$$

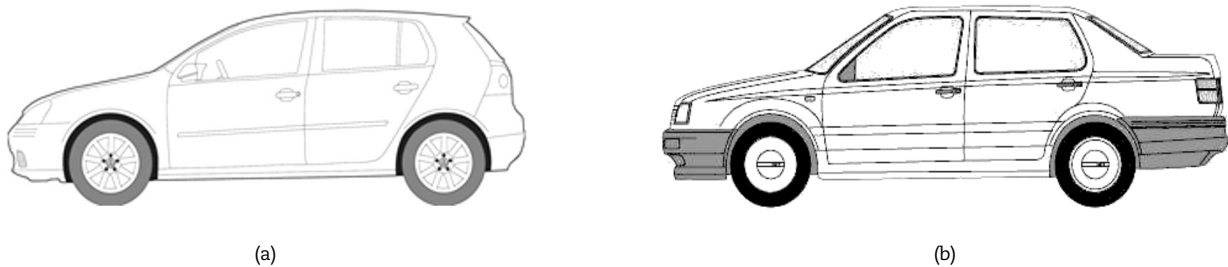


Fig. 1. (a) Hatchback model [33], (b) Sedan model [34].

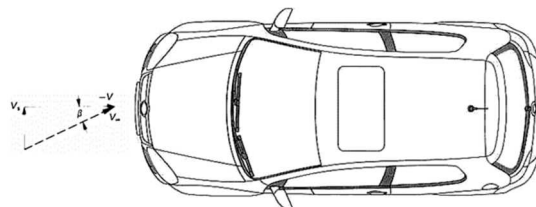


Fig. 2. Definition of yaw angle.

Table 1. Dimensions of hatchback and sedan models and computational domain [33, 34]

Dimensions (mm)	Hatchback	Sedan	Computational domain
Length	4338	4404	40000
Width	1807	1694	3000
Height	1613	1423	3000



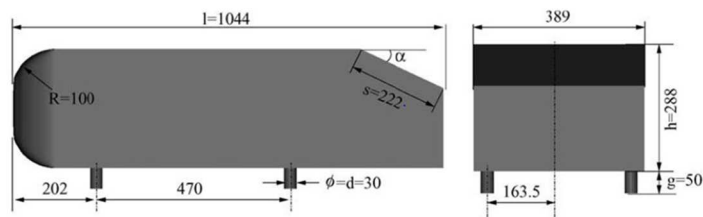


Fig. 3. Ahmed's body geometry [8] (dimensions are in mm).

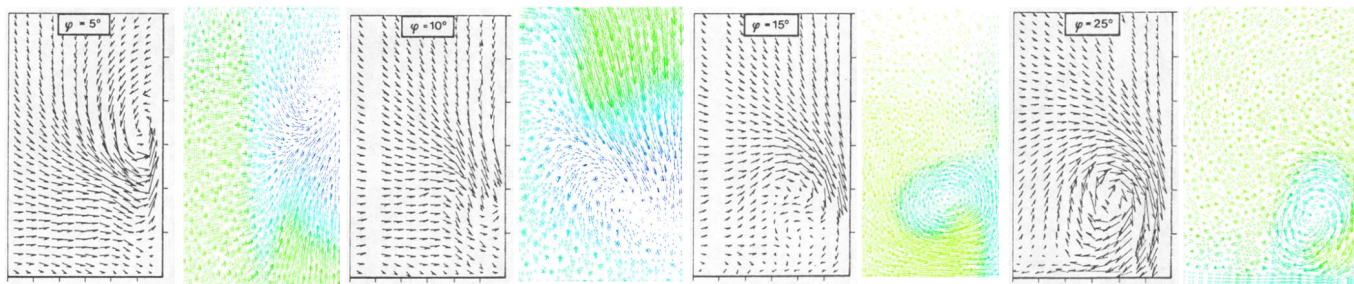


Fig. 4. Comparison of the results of the numerical solution with crossflow velocity distribution for the different base slant of Ahmed et al [8].

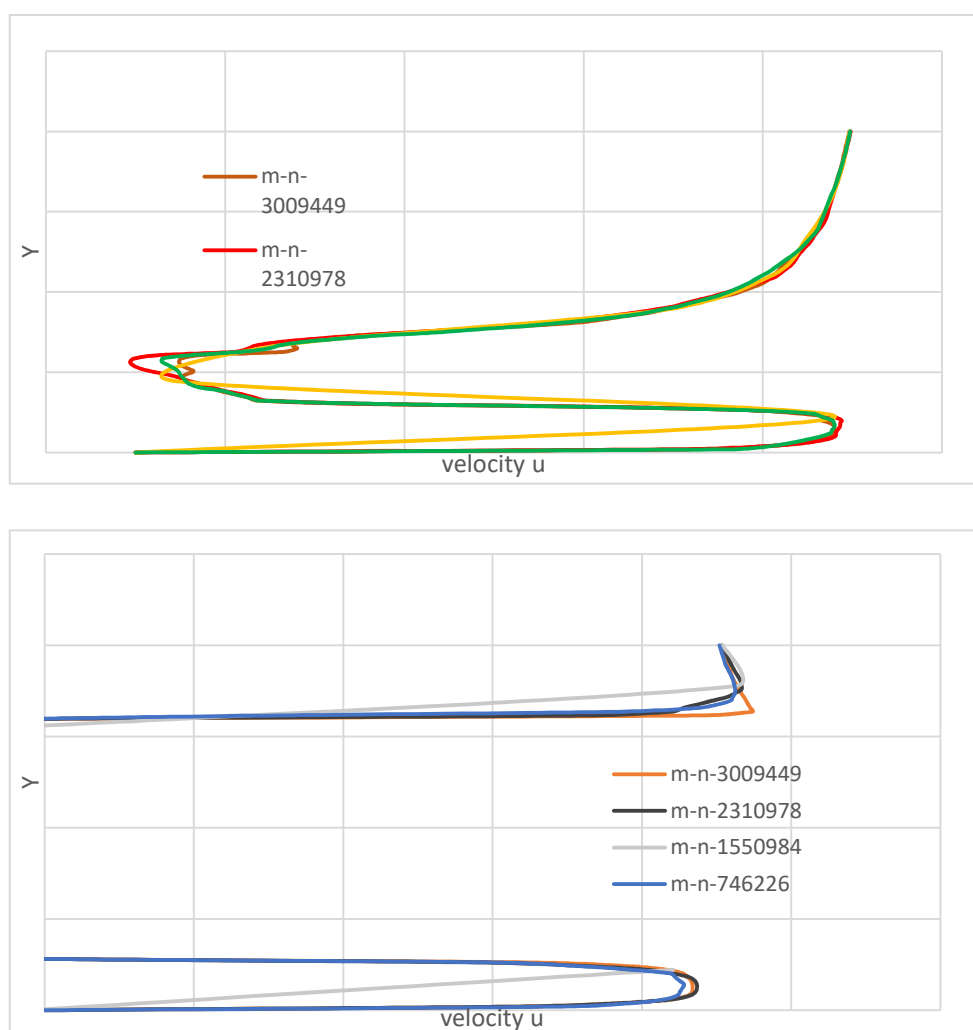


Fig. 5. velocity profiles for the hatchback vehicle in several mesh numbers.



3.1 Numerical Simulation

The flow is three-dimensional and steady; the equations of momentum and turbulence model are discretized by the use of the second-order upwind method. The boundary conditions are defined as follows: The air enters the computational domain at 40 m/s; at the exit, the air pressure is considered atmospheric pressure. Given that half of the computational domain is considered, the gradient of all parameters perpendicular to the symmetry boundary is considered as zero. For the other lateral wall and the upper boundary of the computational domain, the symmetry boundary condition is applied. The lower wall of the computational domain, as well as the walls of the vehicle, are considered as the no-slip wall boundary. In the case of lateral wind effects, the vehicle speed is 40 m/s and the wind speed is 10 m/s, perpendicular to the main flow. Turbulent intensity is 1% and turbulent viscosity ratio is 10.

3.2 Validation

The flow around a geometry that is called "Ahmed body" has been considered. This geometry and its details, which are shown in Fig. 3. In Fig. 4, the results of the present numerical simulation are compared with the experimental results of Ahmed et al [8] in various angles of the back of the body. As shown in this figure4, the results of the numerical solutions are well-matched with the available experimental data.

3.3 Computational domain

The tetragonal mesh with inflation layers is utilized. The velocity profiles for the hatchback vehicle with a spoiler at the angle of 0° and the length of 300 mm in terms of the number of meshes are in two different areas shown in Fig. 5. As shown in this figure, there is no particular change in the results in the number of meshes up to more than 1.5 million. Hence, to ensure mesh independence, the number of meshes is selected at about 3 million. Figure 6 shows the computational domain for both sedan and hatchback vehicles with several meshes of about 3 million for both cars.

4. Results

In this section, flow over the hatchback and the sedan cars are simulated numerically; these cars are simulated as manufactured forms, with a single spoiler and double spoilers; in addition, effects of cross-flow wind in aerodynamics properties of cars are studied. The cross-flow over vehicles is considered as 10 m/s perpendiculars to the main axis of the car.

4.1 Discussion

In this section, the results of flow simulation for hatchback and sedan cars are discussed in detail. In all figures of this part, for comparison, the coefficient of drag and lift for sedan and hatchback cars in the ordinary and manufactured form are depicted. Figure7 shows the variations of the drag coefficient for hatchback and sedan cars in different spoiler types and angles. From the curves of this figure, we can conclude as follow. For the hatchback car with a single spoiler and angle of the spoiler less than ten degrees. In contrast, increasing the spoiler angle greater than 10 degrees increases the coefficient of drag. For the hatchback car with two spoilers, the drag coefficient is almost constant. For the sedan car with a single spoiler, the angle increasing of the spoiler increases the drag coefficient but it decreases slightly at 50° . Drag coefficients for the sedan with two spoilers indicate that this design is not suitable for the sedan vehicle especially for angles of 10 and 30 degrees.

Figure 8 shows the negative pressure, $c_p < 0$, is present on almost the entire rear end without a spoiler while the spoiler creates positive pressure, $c_p > 0$, over a large area, this result is compatible with Ohtani et al. [37]; moreover, the pressure at the front of the car remains unchanged by the rear spoiler, although the pressure at the rear end is increased even in the area of the wake which is due to the reduction in rear flow field curvature as the spoiler deflect the vortex-generated down-wash flow. The net drag change due to the rear spoiler is primarily a result of the opposing trends of drag reductions on rear surfaces and drag increases on the spoiler and rear underbody area. Decreases in underbody pressures, as well as the pressure drop across the spoiler itself, will generate drag increases which may partially or completely cancel gains on the back, Schenkel [38].

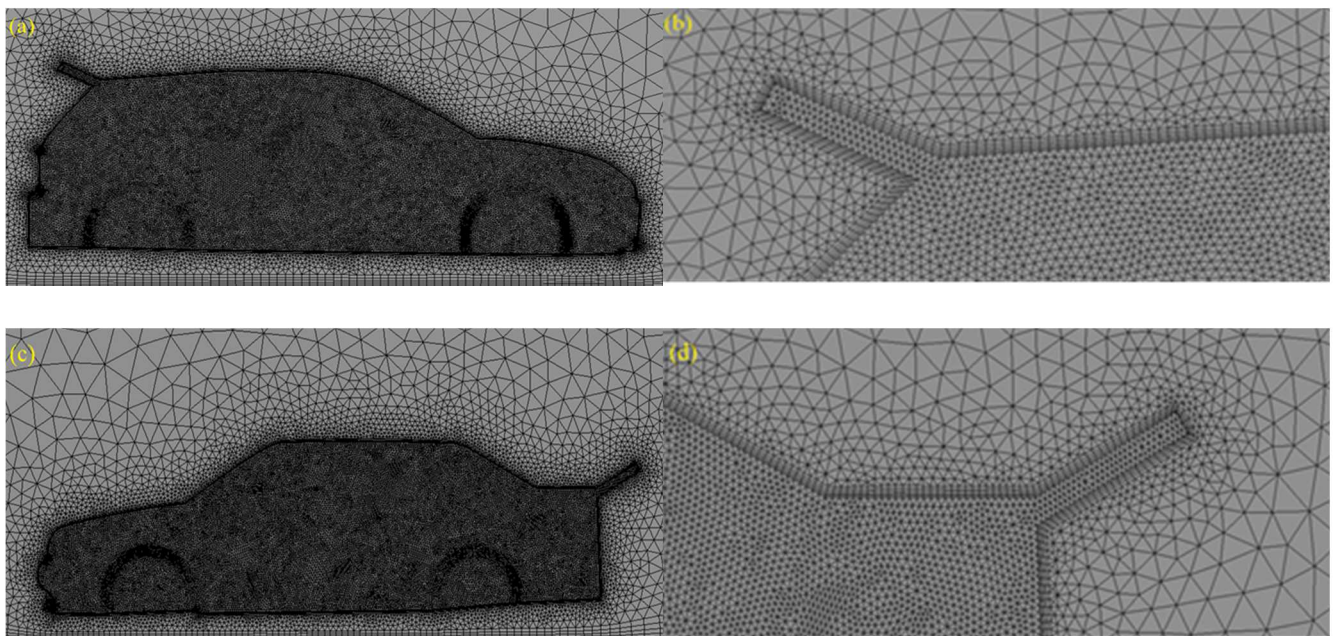


Fig. 6. a) Distribution of the mesh around the hatchback car, b) a close view of the inflation layers of the hatchback car, c) distribution of the mesh around the sedan car, d) a close view of the inflation layers around the sedan car.



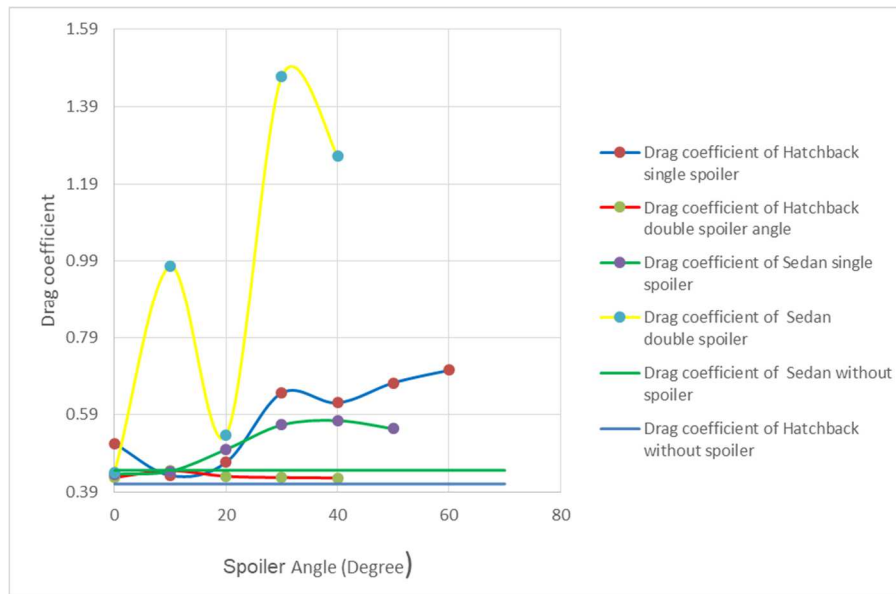


Fig. 7. Drag coefficient variations by changing the spoiler angle for hatchback and sedan cars without crosswind.

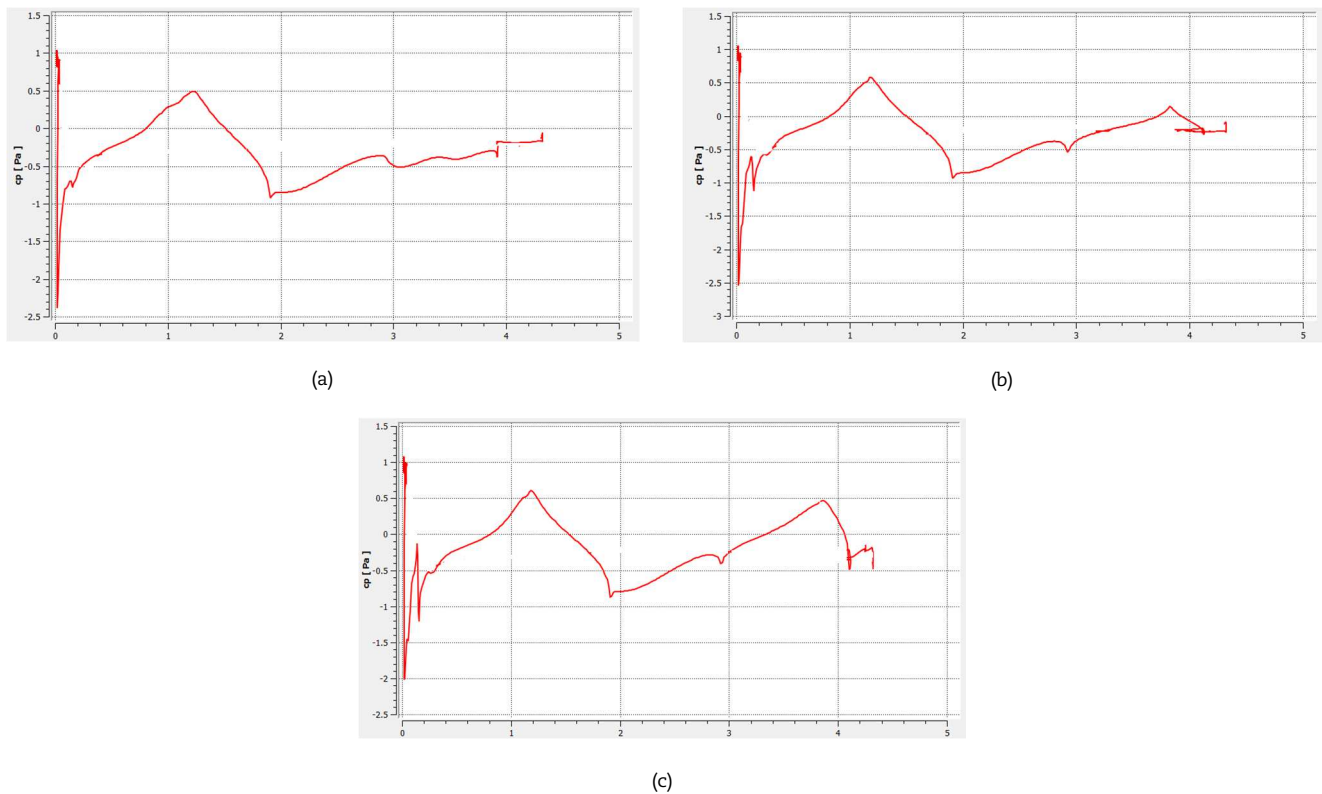


Fig. 8. Pressure coefficient on the surface of hatchback car a) without a spoiler, b) 10 degrees spoiler, and c) 30 degrees spoiler.

Figure 9 shows the variations of the drag coefficient for hatchback and sedan cars by changing the angle of the spoiler with the crosswind. Almost for all cases, with increasing the spoiler angle, pressure diffraction between the front of the car and its back increase; consequently, it causes to increase in the drag coefficient. Except for sedan cases with a double spoiler which has fluctuated pattern shown in fig 10. This is because while for all cases with increase spoiler degree, these diffraction increase, for 30-degree spoiler this has the opposite influence. Therefore, the drag pattern fluctuates. For the Hatchback vehicle, the drag coefficient increases continuously at zero angles to 50 degrees in comparison with the hatchback car without a spoiler. For the sedan with a single spoiler, in zero up to 10 degrees, the coefficient of drag decreases in contrast without a spoiler. By adding the rear spoiler to both cars, the largest reduction in the drag coefficient of the sedan is related to the 0-degree spoiler angle with 36% lower drag, compared to the no-spoiler mode; for the hatchback car, the biggest drag reduction is about 43% at 0 degrees spoiler angle. By adding a roof spoiler simultaneously with the rear spoiler, for the sedan car, the 30-degree angle of the spoiler causes to reduce the drag coefficient up to 21 percent; it is the best condition; and for the hatchback vehicle, with the spoiler at a 0-degree angle, decrease the drag coefficient up to 7 percent.



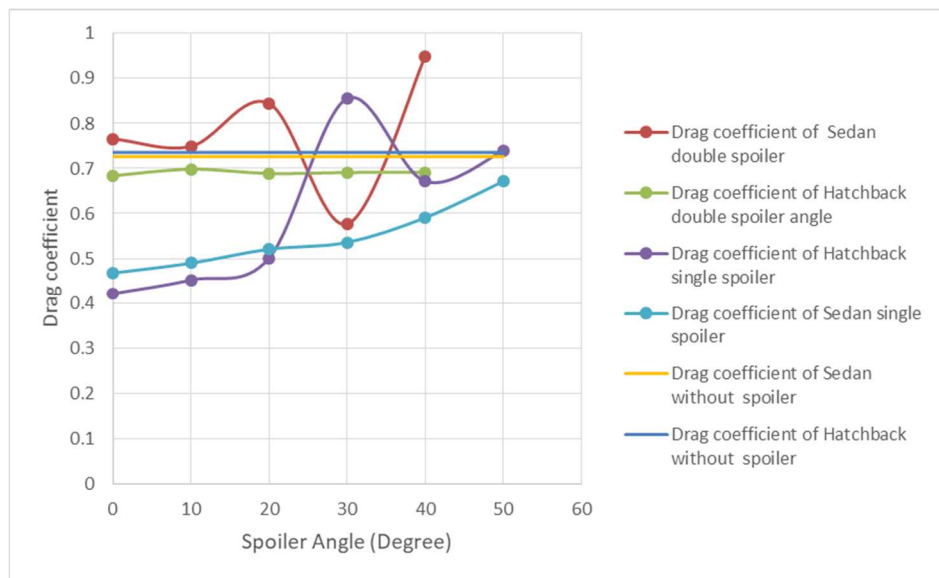


Fig. 9. Drag coefficient variations versus changing the spoiler angle for hatchback and sedan cars with the crosswind.

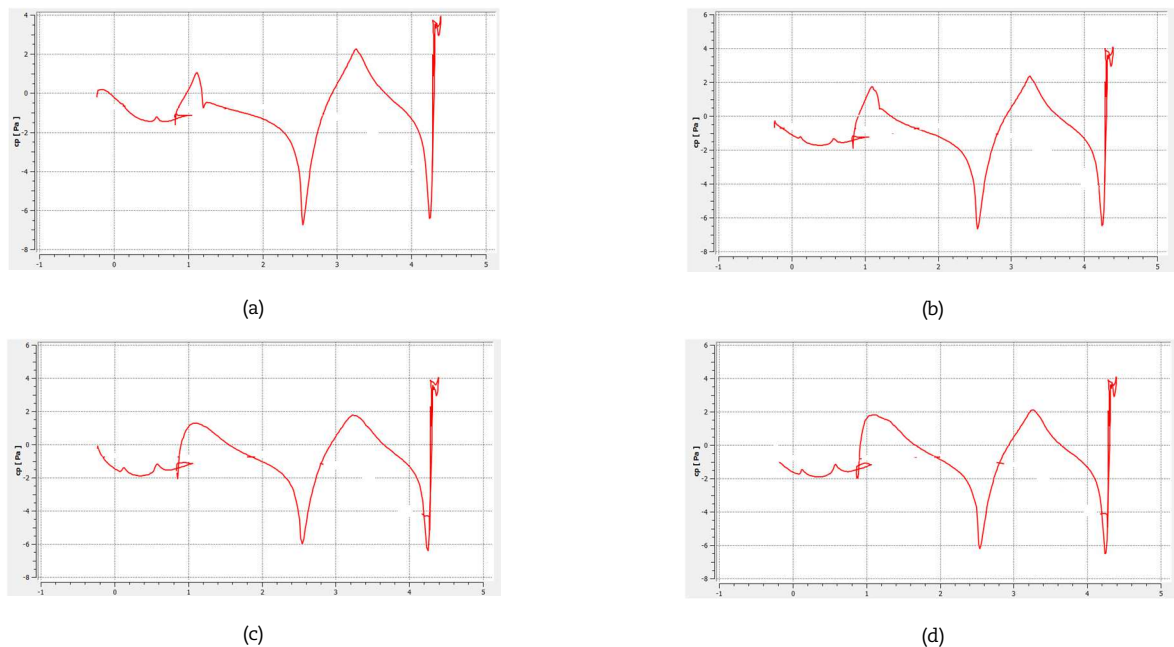


Fig. 10. Pressure coefficient on the surface of sedan car a) 10 degrees spoiler, b) 20 degrees spoiler, c) 30 degrees spoiler, d) 40 degrees spoiler.

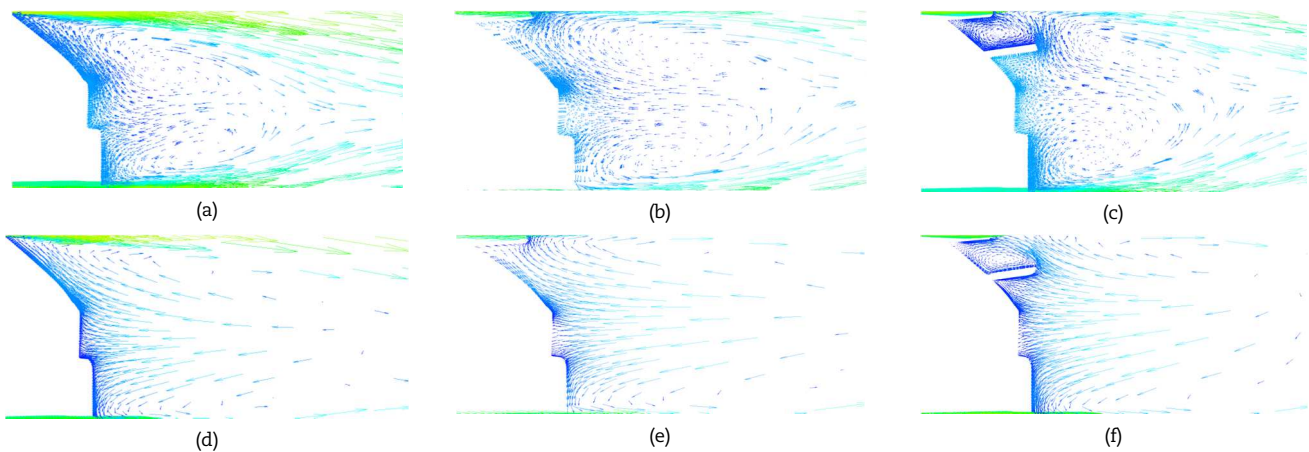


Fig. 11. The numerical predictions of the streamlines superimposed with velocity contours in the x-y plane for (a,d) the Hatchback without a spoiler, (b,e) the Hatchback with a single spoiler, and (c,f) the Hatchback with doubler spoiler under crosswind.



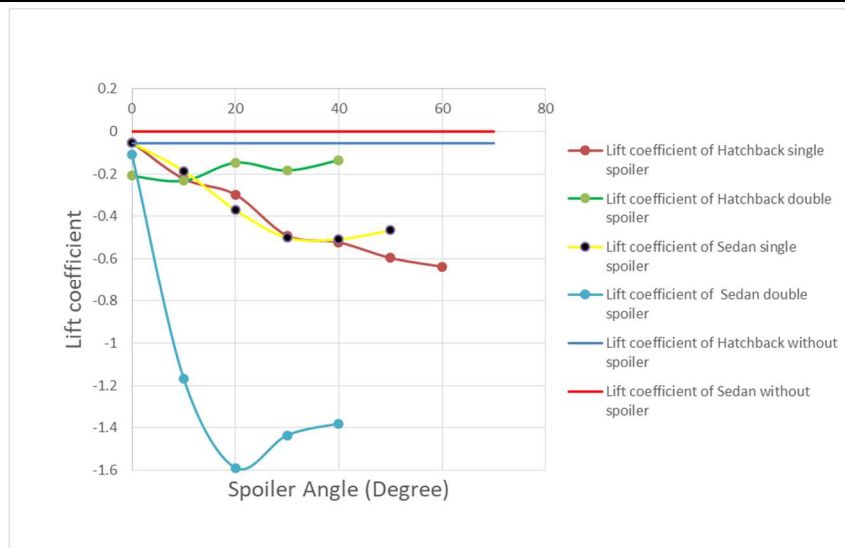


Fig. 12. Lift coefficient variations by changing the spoiler angle for hatchback and sedan cars without crosswind.

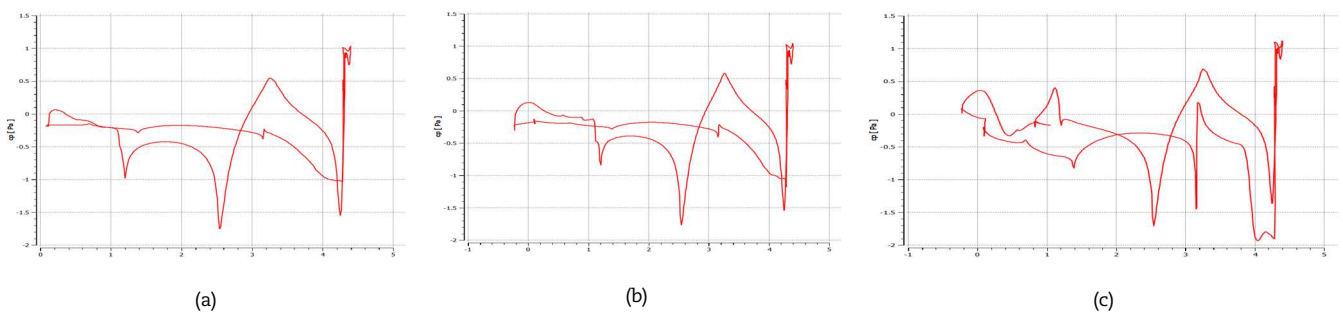


Fig. 13. Pressure coefficient on the surface of sedan car a) without a spoiler, b) 10 degrees spoiler, and c) 10 degrees double spoiler.

The near-wake structure for the Hatchback is shown for 3 cases in Fig. 11 under crosswind. The sections closer to the leeward edge (a-c), closer to the windward edge (d-f). Section-wise, the wake structure exhibited by the Hatchback without a spoiler in Fig. 11 (a,d), the Hatchback with a single spoiler in Fig. 11 (b,e), and the Hatchback with double spoiler in Fig. 11 (c,f) are different but such differences appear to be minimal. With the Hatchback without a spoiler, the flow is initially attached closer to the roof-slant edge for the windward edge but significantly detaches further downstream, and as a consequence, a distinctively deformed wake structure is seen with the Hatchback without a spoiler in Fig. 11 (e), wherein closer to the leeward side it is characterized by massive separation over the slant, like just the recirculation zone that is exhibited by other the models.

Figure 12 shows the variations of lift coefficient around the hatchback and sedan vehicles without crosswind. The value of the lift coefficient for all angles is negative, the downward force increases, in view of the fact that the stability of cars is improved. In addition, this figure shows the inappropriateness of the design of the sedan car with two spoilers, because of the fact that there are high downward forces for some angles.

Figure 13 illustrates that the spoiler attached to the rear end of the car interrupts the smooth streamline airflow thereby slowing down the airflow and correspondingly raising the upper surface local air pressure which effectively increases the downward force known as negative lift, Schenkel [38]. Surprisingly, the rear spoiler not only changes the pressure on the top of the vehicle, where it causes a pressure increase, but the pressure on the underside is decreased, Hucho [9].

In Fig. 14, the variations of coefficient of lift for the Hatchback and the Sedan vehicles with crosswind are shown. Almost for all cases, with an increase of angle of the spoiler, the lowering coefficient of lift is reduced, because of the fact that the negativity of the coefficient of lift, it can be concluded that the stability of the cars increases. In the case of one rear spoiler, the maximum increase in the negative lift coefficient for the Sedan car at the 50-degree angle spoiler is 0.4794; also for the Hatchback car, the maximum increase in the negative lift coefficient at the 30-degree angle is 0.7206, compared to the no-spoiler mode. In the case of the roof spoiler with the rear spoiler, for the sedan car, at the 40-degree angle of the spoiler, the negative lift coefficient is 0.3714 and for the Hatchback car at the 20-degree is 0.3980.

Figure 15 shows the variation of drag coefficient around the hatchback and the sedan vehicles with single spoiler versus different spoiler lengths with and without crosswind. In the case of crosswind, for the hatchback car, from 200 mm to 300 mm of spoiler length, the drag coefficient decreases, but by increasing the length of spoiler from 300 mm, the increase in spoiler length, causes less pressure and crosswind vortices, as a result, the drag coefficient increases. In the sedan car and with a crosswind, by increasing the spoiler length from 200 mm to 500 mm, the drag coefficient is increased. As the rear spoiler lengths increase, for the sedan car, the 300 mm long spoiler decreases the drag coefficient by 33%, and the 300 mm long spoiler reduces the drag coefficient by 27% for the hatchback car.

The aerodynamic drag force slowly increases because of the alter in pressure between the front and rear of the vehicle, which can be explained by the pressure coefficient distribution on the upper surface of the vehicle. When the vehicle moves forward, the air within the front of the car is pushed, increasing the pressure acting on the front of the car. In the meantime, the negative pressure is created by the wake in the rear of the car, which diminishes the pressure acting on the rear of the car. The pressure difference between front and back forms pressure resistance. Figure 16 shows that the front and rear pressure difference at crosswind conditions is larger than that without a crosswind situation, resulting in an increase in drag force, Zhang et al. [39].



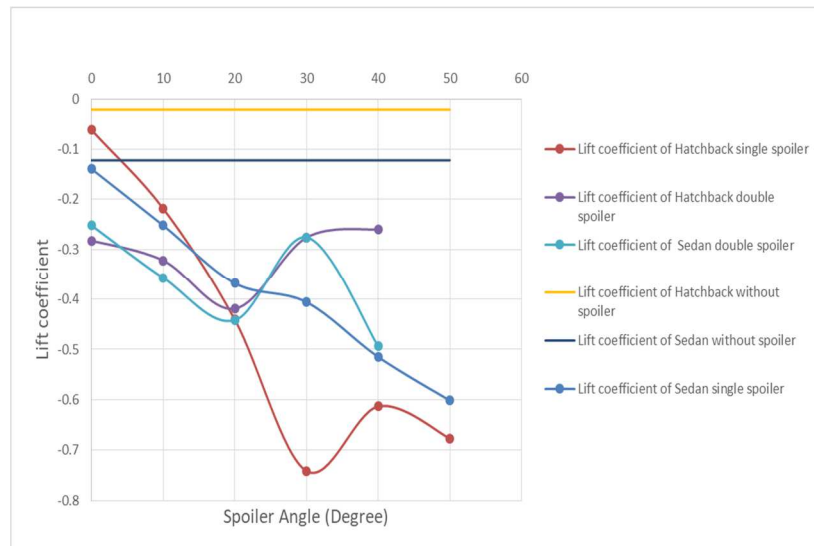


Fig. 14. Lift coefficient variations by changing the spoiler angle for hatchback and sedan cars with the crosswind.

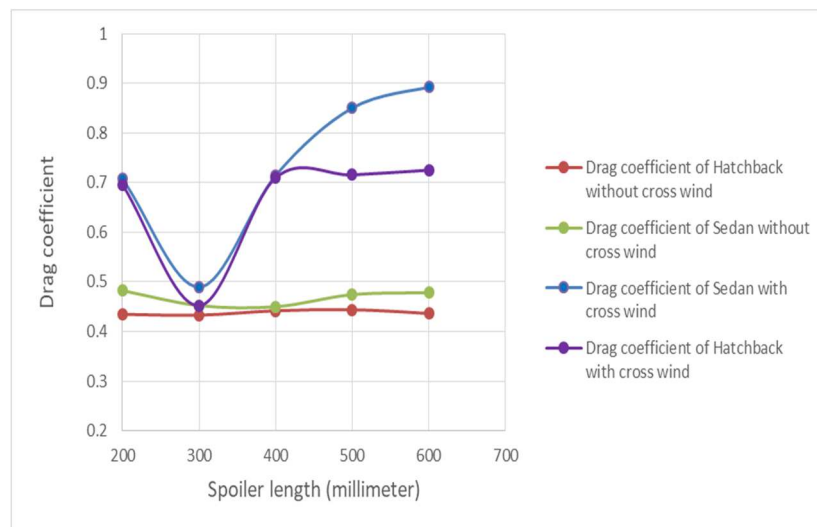


Fig. 15. Drag coefficient variations versus the spoiler length for the hatchback and the sedan cars with a crosswind and without crosswind.

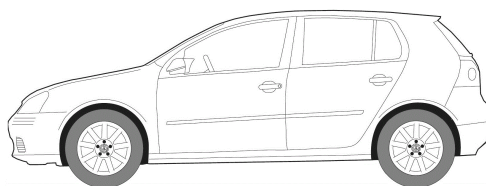
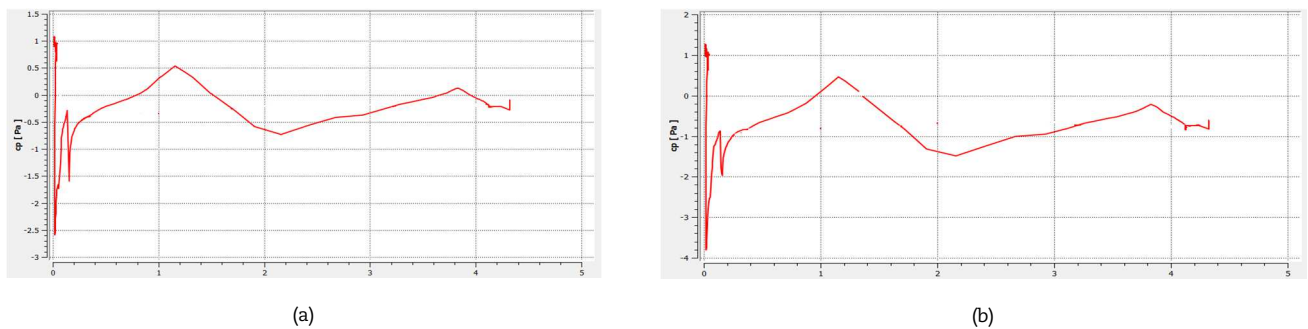


Fig. 16. Pressure coefficient on the surface of the vehicle: (a) the spoiler without crosswind, (b) the spoiler case under crosswind.

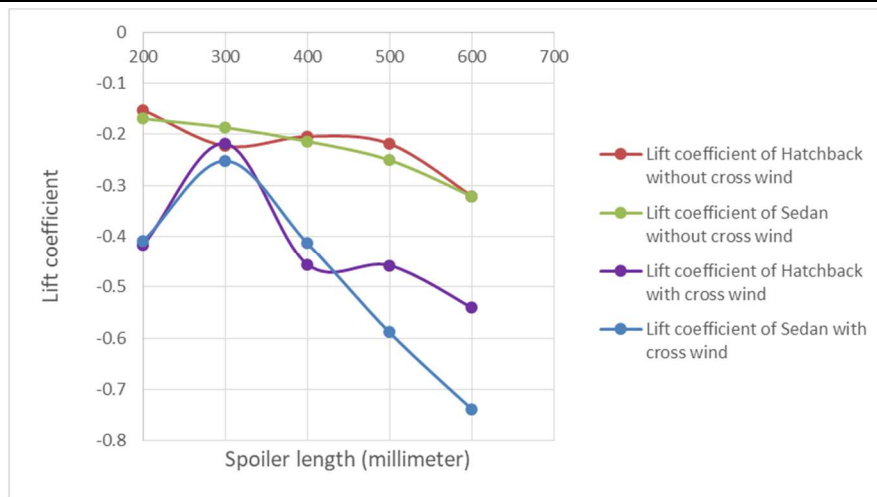


Fig. 17. Lift coefficient variations by changing the spoiler length in the hatchback and the sedan cars with and without crosswind.

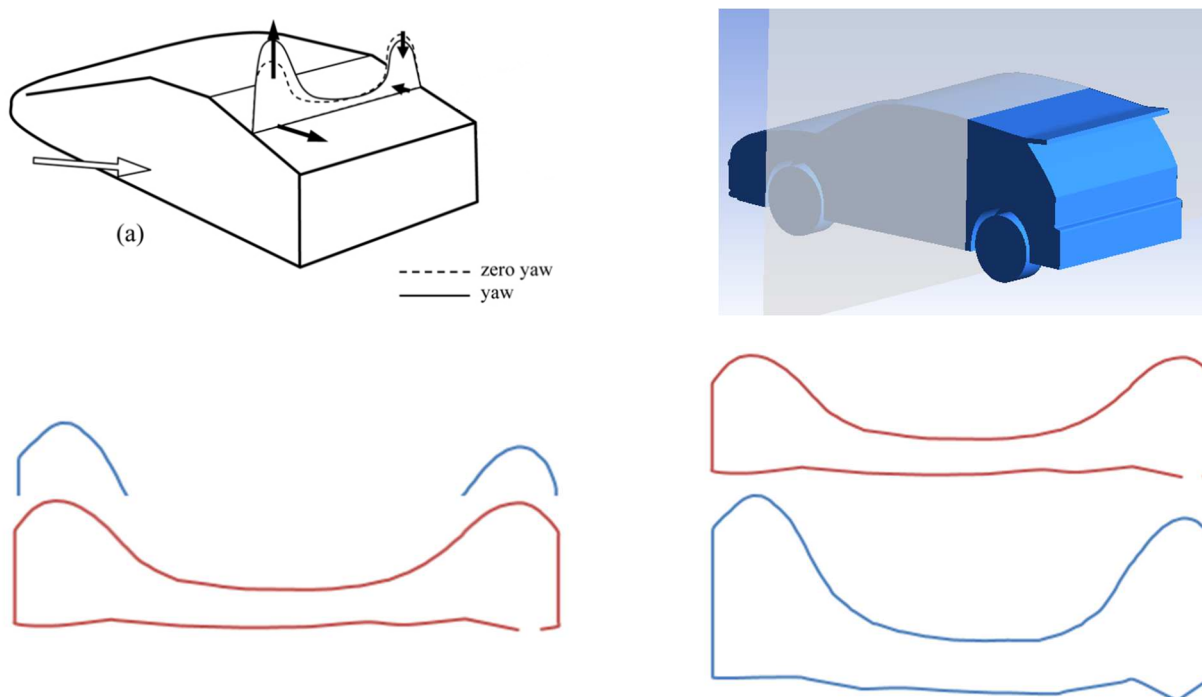


Fig. 18. Sketches showing the effect of yaw on the pressure distributions on the sloping backlight surface
red: without a side force condition, blue: side force condition.

Figure 17 depicts the variation of lift coefficient for the hatchback and the sedan vehicles with a single spoiler, in different lengths with and without crosswind. The lift coefficient is negative for all lengths; therefore, the force is downward. With the increase in rear spoiler length for both cars, the best negative coefficient of lift for the sedan becomes -0.6160 in the 600 mm long spoiler, and in addition to the hatchback car, for the 600 mm spoiler size, the negative lift coefficient becomes -0.5192. For the hatchback vehicle, with increasing the spoiler length, in the first step, the lift coefficient decreases and after that, it increases. For the sedan car, with the increase in the length of the spoiler, the lift coefficient always decreases.

Figure 18 shows the effect of yaw on the pressure distributions on the sloping backlight surface. Moreover, the side force causes a lee-ward steering effect. This is lead to decrease suction in the vortex on the windward side and an opposite trend in the lee side vortex. On the windward side, an increase in pressure coefficient can be seen along the inclined edge, whereas on the lee side a decrease in the pressure coefficient as well as suction increase. This is led to the decline of the lift. Howell et al. [40].

5. Conclusion

In this study, the three-dimensional and incompressible airflow was solved for two sample models of sedan and hatchback cars without and with spoilers; the equations of continuity, momentum, and the Realizable $k-\epsilon$ turbulence model were solved by finite volume method. For both models, the angle and length of the spoilers were changed. In addition, the effect of the simultaneous presence of two spoilers, where the angle of one is constant and the other angle is variable, was investigated. All of the mentioned cases were simulated without and with crosswind flow. The velocity vectors around the car in different modes of spoiler installation, different angles, and different lengths were provided; Moreover, in the event that the effects of the crosswind are neglected, the drag coefficients were presented for each case. The increase of the spoiler angle can cause to negative lifting force and greater



stability. Furthermore, increasing the length of a spoiler for the hatchback vehicle up to 400 mm can reduce the drag force slightly, in contrast, does not have much effect on the drag coefficient of the sedan car. The increase of spoiler length for both sedan and hatchback vehicles can increase the downward force and vehicle stability. Where crosswind effects were considered, increasing the spoiler angle, such as with no crosswind conditions, does not have a significant effect on reducing drag force and in some cases, it increases the drag force on both cars. For the sedan car, in single spoiler mode 0° angle and 300 mm length of the spoiler, in double spoiler mode, 30° angle have the lowest drag coefficient; 50° angle, 600 mm length and 40° angle respectively have the highest negative lift coefficient. In addition, for the hatchback car, in single spoiler mode 0° angle and 300 mm length, in double spoiler mode, 0° angle has the lowest drag coefficient and 30° angle, 600 mm length and 20° angle respectively have the highest negative lift coefficient.

Author Contributions

All authors contributed equally to the paper. The manuscript was written through the contribution of all authors. All authors discussed the results, reviewed, and approved the final version of the manuscript.

Acknowledgments

The authors thank the reviewers and editor for the constructive comments. The authors would like to thank the Vice-chancellor for research, Shahid Chamran University of Ahvaz (Grant number: SCU.EM98.376).

Conflict of Interest

The authors declared no potential conflicts of interest concerning the research, authorship, and publication of this article.

Funding

The authors received no financial support for the research, authorship, and publication of this article.

Data Availability Statements

The datasets generated and/or analyzed during the current study are available from the corresponding author on reasonable request.

Nomenclature

\bar{u}	Time-averaged velocity [m/s]	S_{ij}	Rate of the strain tensor [s^{-1}]
ρ	Density [kg/m^3]	\bar{p}	Time average pressure [N/m^2]
μ	Viscosity of fluid [$kg/m.s$]	k	Turbulence kinetic energy, [$m^2.s^{-2}$]
ε	Rate of dissipation of kinetic energy [m^2/s^3]	σ_k	The Prandtl number of the kinetic energy of turbulence
σ_ε	The Prandtl number of rate of dissipation of kinetic energy	P_k	The turbulence kinetic energy production concerning the mean velocity gradient
$C_1, C_{1\theta}, C_2, C_{3\theta}$	Turbulence constants moduli		


References


- [1] Ahmed, S.R., An experimental study of the wake structures of typical automobile shapes, *J. Wind Eng. Ind. Aerodyn.*, 9, 1981, 49–62.
- [2] Wood, R.M., Bauer, S., Simple and Low-Cost Aerodynamic Drag Reduction Devices for Tractor-Trailer Trucks, *SAE International Truck and Bus Meeting and Exhibition*, Texas, USA, 2003-01-3377, 2003.
- [3] White, F.M., *Fluid mechanics*, McGraw-Hill, New York, 2011.
- [4] Katz, J., Aerodynamics of Race Cars, *Annu. Rev. Fluid Mech.*, 38, 2006, 27–63.
- [5] Gilliéron, P., Kourta, A., Aerodynamic drag reduction by vertical splitter plates, *Exp. Fluids*, 48, 2010, 1–16.
- [6] Rojewski, A., Bartoszewicz, J., Numerical analysis of influence of the wing in ground effect on aircraft lift coefficient and on car downforce coefficient, *J. Mech. Transp. Eng.*, 69, 2017, 47–54.
- [7] Katz, J., *Race Car Aerodynamics Designing for Speed Engineering and Performance*, Bentley Publishers, 1995.
- [8] Ahmed, S.R., Ramm, G., Faltin, G., Some salient features of the time-averaged ground vehicle wake, *SAE Technical Paper*, 1984, 1-34.
- [9] Crabtree, L.F., Aerodynamics of Road Vehicles, *Aeronat. J.*, 91(906), 1987, 285–285.
- [10] Ranzenbach, R., Barlow, J.B., Diaz, R.H., Multi-element airfoil in ground effect- an experimental and computational study, *15th Applied Aerodynamics Conference*, USA, 1997.
- [11] Kim, M.H., Numerical study on the wake flow characteristics and drag reduction of large-sized bus using rear-spoiler, *Int. J. Veh. Des.*, 34, 2004, 203–217.
- [12] Kieffer, W., Moujaes, S., Armbya, N., CFD study of section characteristics of Formula Mazda race car wings, *Math. Comput. Model.*, 43, 2006, 1275–1287.
- [13] Fares, E., Unsteady flow simulation of the Ahmed reference body using a lattice Boltzmann approach, *Comput. Fluids*, 35, 2006, 940–950.
- [14] Hargreaves, D.M., Morvan, H.P., Wright, N.G., CFD modeling of high-sided vehicles in cross-winds, *Fourth Int. Symp. Comput. Wind Eng.*, 2006.
- [15] Chainani, A., Perera, N., CFD investigation of airflow on a model radio control race car, *WCE*, London, UK, 2008.
- [16] Tsai, C.H., Fu, L.M., Tai, C.H., et al., Computational aero-acoustic analysis of a passenger car with a rear spoiler, *Appl. Math. Model.*, 33, 2009, 3661–3673.
- [17] Mitra, D., Effect of relative wind on notch back car with add-on parts, *Int. J. Eng. Sci. Technol.*, 2, 2010, 472–476.
- [18] Tsubokura, M., Nakashima, T., Kitayama, M., et al., Large eddy simulation on the unsteady aerodynamic response of a road vehicle in transient crosswinds, *Int. J. Heat Fluid Flow*, 31, 2010, 1075–1086.
- [19] Hu, X., Wong, E.T., Numerical study on rear-spoiler of passenger vehicle, *Int. J. Mech. Aerospace*, 57, 2011, 636–641.
- [20] Zhu, L.D., Li, L., Xu, Y.L., et al., Wind tunnel investigations of aerodynamic coefficients of road vehicles on bridge deck, *J. Fluids Struct.*, 30, 2012, 35–50.
- [21] Sadettin, H., Salah R., Aydin, M., et al., Effects of rear spoilers on ground vehicle aerodynamic drag, *Int. J. Numer. Methods Heat Fluid Flow*, 24, 2014, 627–642.
- [22] Sung, L.G., Wan, W.Z., Zainudin, A.Z., et al., Aerodynamic Analysis of the Preliminary Design of SURIKAR 4 Using CFD, *Appl. Mech. Mater.*, 629, 2014, 507–512.




- [23] Bahoosh, R., Momenifar, M., INVESTIGATION OF AERODYNAMIC FORCES ON TWO TANDEM CARS, *International Symposium on Convective Heat and Mass Transfer*, Kusadasi, Turkey, 2014.
- [24] Cheng, S.Y., Mansor, S., Influence of rear-roof spoiler on the aerodynamic performance of hatchback vehicle, *Fifteenth Asian Congress of Fluid Mechanics*, Sarawak, Malaysia, 2016.
- [25] Liu, X., Han, Y., Cai, C.S., et al., Wind tunnel tests for mean wind loads on road vehicles, *J. Wind Eng. Ind. Aerodyn.*, 150, 2016, 15–21.
- [26] Mashud, M., Rubel, C.D., Effect of rear end spoiler angle of a sedan car, *AIP Conference Proceedings*, Dhaka, Bangladesh, 2017.
- [27] Li, T., Zhang, J., Rashidi, M., Yu, M., On the Reynolds-Averaged Navier-Stokes Modelling of the Flow around a Simplified Train in Crosswinds, *J. Appl. Fluid Mech.*, 12, 2019, 551–563.
- [28] Ferraris, A., Airale, A.G., et al., City Car Drag Reduction by Means of Shape Optimization and Add-On Devices, *IFTOMM World Congress on Mechanism and Machine Science*, Krakow, Poland, 2019.
- [29] Yıldız, A., Dandil, B., Investigation of effect of vehicle grilles on aerodynamic energy loss and drag coefficient, *J. Energy Syst.*, 2, 2018, 190–203.
- [30] Guo, H.L., Qin, P.P., Cui, R.Y., Using the numerical simulation analyzes the influence of the rear wing on the Car's aerodynamic, *ACM International Conference Proceeding Series*, New York, USA, 2008.
- [31] Prakash, S., Parth, N.B., et al., Prototype Development of Car By Improving Aerodynamic Shapes & Calculation of Aerodynamic Forces, *J. Nov. Res. Dev.*, 2018, 82–86.
- [32] Džijan, I., Pašić, A., Buljac, A., et al., Aerodynamic forces acting on a race car for various ground clearances and rake angles, *J. Appl. Fluid Mech.*, 12, 2019, 361–368.
- [33] <https://drawingdatabase.com/volkswagen-golf-v/>, 7/20/2019.
- [34] https://www.the-blueprints.com/blueprints/cars/vw/24715/view/volkswagen_jetta_1993_/, 7/20/2019.
- [35] Launder, B.E., Sharma, B.I., Application of the energy-dissipation model of turbulence to the calculation of flow near a spinning disc, *Lett. Heat Mass Transf.*, 1, 1974, 131–137.
- [36] Jones, W., Launder, B., The prediction of laminarization with a two-equation model of turbulence, *Int. J. Heat Mass Transf.*, 15, 1972, 301–314.
- [37] Ohtani, K., Takei, M., Sakamoto, H., Nissan Full Scale Wind Tunnel—Its Application to Passenger Car Design, *SAE Technical Paper*, 1972, 1018–1030.
- [38] Schenkel, F.K., The Origins of Drag and Lift Reductions on Automobiles with Front and Rear Spoiler, *SAE Technical Paper*, 1977, 1661–1671.
- [39] Zhang, Q., Su, C., Wang, Y., Numerical investigation on aerodynamic performance and stability of a sedan under wind-bridge-tunnel road condition, *Alexandria Eng. J.*, 59, 2020, 3963–3980.
- [40] Howell, J., Fuller, J.B., A Relationship between Lift and Lateral Aerodynamic Characteristics for Passenger Cars, *SAE Technical Paper*, 2010, 1025–1036.

ORCID iD

Reza Bahoosh  <https://orcid.org/0000-0001-9609-052X>

Milad Rohani  <https://orcid.org/0000-0002-2725-4233>

Mohammad Reza Saffarian  <https://orcid.org/0000-0003-0326-0505>



© 2022 Shahid Chamran University of Ahvaz, Ahvaz, Iran. This article is an open access article distributed under the terms and conditions of the Creative Commons Attribution-NonCommercial 4.0 International (CC BY-NC 4.0 license) (<http://creativecommons.org/licenses/by-nc/4.0/>).

How to cite this article: Bahoosh R., Rohani M., Saffarian M.R. Numerical Simulations of Spoiler's Effect on a Hatchback and a Sedan Car Exposed to Crosswind Effect, *J. Appl. Comput. Mech.*, 9(2), 2023, 346–356.
<https://doi.org/10.22055/JACM.2021.36955.2937>

Publisher's Note Shahid Chamran University of Ahvaz remains neutral with regard to jurisdictional claims in published maps and institutional affiliations.

